Passive radar using Global System for Mobile communication signal: theory, implementation and measurements

D.K.P. Tan, H. Sun, Y. Lu, M. Lesturgie and H.L. Chan

Abstract: Passive radars using illuminators of opportunity have attracted much attention in the international radar community. One existing radio transmission system that may be utilised for this purpose is the Global System for Mobile communication (GSM). The paper presents a study showing the feasibility of using a GSM signal for passive radar. The analysis of the GSM waveform, and any significance or influence it has with respect to the passive radar design considerations are investigated in detail. The paper describes fully the design and implementation of a low-cost GSM-based passive radar prototype in addition to the associated signal processing scheme. Numerous measurements for various ground-moving targets were investigated extensively. The preliminary processing results demonstrate the feasibility of using GSM signals as a radar waveform and have the potential capability to detect and track different types of ground-moving targets.

1 Introduction

Passive radar is, essentially, a receiver-only radar that usually dissociates the receiving antenna at a different location from the transmitter. Containing no transmitter, the benefits that a passive radar can offer are numerous. Most importantly, passive radar is virtually undetectable to surveillance receivers and there is also no constraint in spectrum allocation. In most cases, passive radar is smaller, more portable and is of lower cost compared to conventional active radar. In recent years, passive radar, using the non-cooperative illuminators of opportunity, has attracted more and more attention from the international radar community [1]. FM radio, TV broadcast, and satellite-borne communication signals have already been used, or considered as, a radar waveform [2–6].

One existing radio transmission system suitable for passive radar operation is the Global System for Mobile communication (GSM). GSM base stations are honeycombed across large areas, transmitting and receiving streams of radio signals to provide continuous service for users. This transmitter-rich communication system is a valuable resource for passive radar with at least two distinct advantages. First, illuminators of such transmissions are abundant. Second, multiple base stations can be utilised in a multistatic passive radar network consisting of multiple passive radar receivers for improving the radar performance and capability. Some preliminary work in this area has been conducted already and can be found in [7–9].

IEE Proceedings online no. 20055038

doi: 10.1049/ip-rsn:20055038

Paper first received 25th June and in revised form 14th December 2004

D.K.P. Tan, H. Sun, Y. Lu and H.L. Chan are with Temasek Laboratories, Nanyang Technological University, Research TechnoPlaza, 8th & 9th Storey, BorderX Block, 50 Nanyang Drive, Singapore 637553

M. Lesturgie is with Office National d'Etudes et de Recherches Aerospatiales (ONERA), France

E-mail: ehbsun@ntu.edu.sg

This paper intends to demonstrate the potential capabilities of GSM-based passive radar for the detection and tracking of various ground-moving targets. To facilitate the research, based on previous work in [8], an improved low-cost experimental GSM-based passive radar was developed at Nanyang Technological University, Singapore. This paper describes fully the complete hardware and associated signal processing schemes of the GSM-based passive radar in addition to experimental results for ground-moving target detection and tracking.

2 Analysis of GSM signal as a radar waveform

2.1 GSM multiple access scheme and channel structure

GSM is a globally-accepted standard for digital cellular communication systems currently in service in most regions of the world. The multiple access scheme in GSM is such that the radio channels are based on a time division multiple access (TDMA) structure that is implemented on multiple frequency sub-bands. Individual base stations are assigned with a certain number of these pre-assigned frequency/time channels. Two frequency bands of 25 MHz each at around 900 MHz (GSM 900) have been allocated for the use in GSM: 890–915 MHz for the uplink and 935–960 MHz for the downlink [10]. In addition, the GSM system in Singapore also operates in the 1800 MHz frequency band (GSM 1800). However, this paper only considers the GSM 900 system.

Each uplink and downlink GSM frequency band is divided into 124 pairs of carriers spaced by 200 kHz. Each carrier is divided into 8 time slots using TDMA. These time slots are used to carry user and signaling/control information in bursts. The bursts are slightly shorter than the slots to allow for burst timing alignment errors, delay dispersion on the path, and for smooth switch on/off of the transmitter. A group of 8 consecutive time slots form a TDMA frame with a duration of 4.615 ms. A transmission channel/burst occupies one time slot position of 577 μs within a TDMA frame. Larger frames are formed from groups of 26 or 51 TDMA frames and the position within such frames defines the type

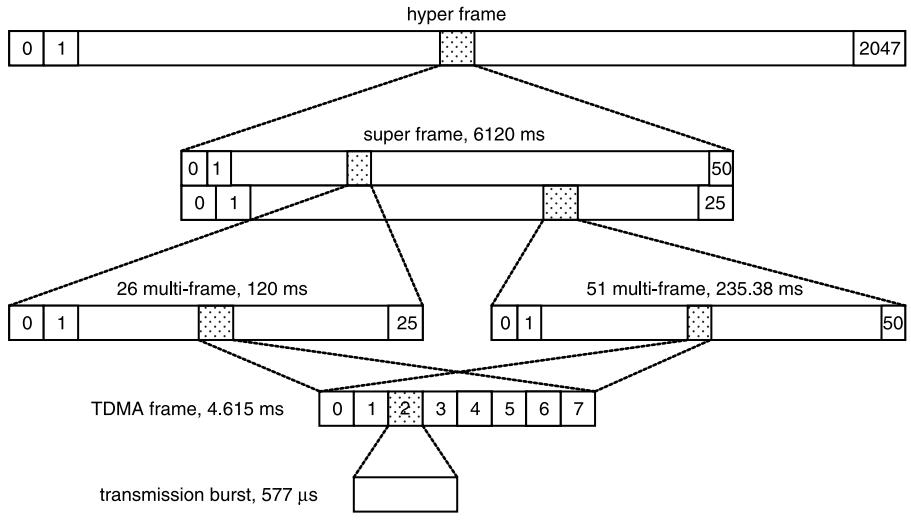

Fig. 1 *GSM radio frame channel hierarchy*

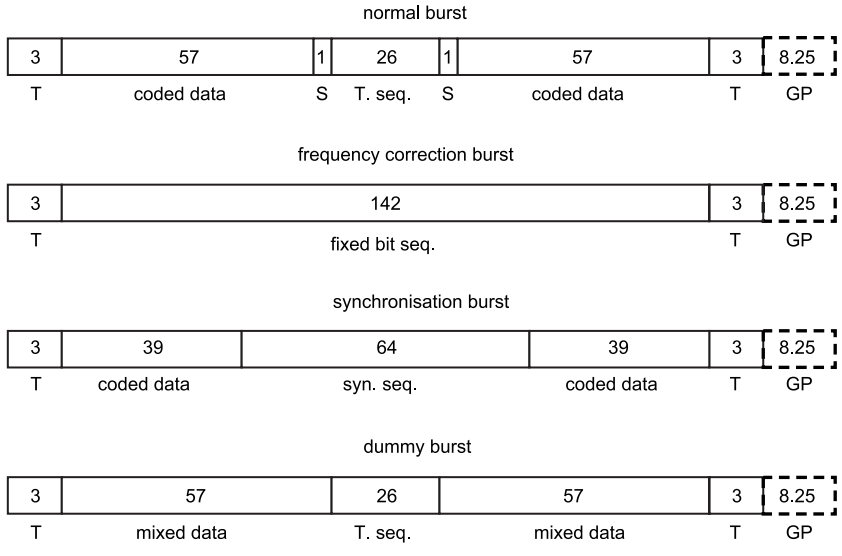

Fig. 2 *Different GSM transmission burst*

and function of a channel. Figure 1 illustrates the GSM frame hierarchical structure [11].

A burst is a period of RF carrier, which is modulated by a data stream. It represents the physical content of a timeslot. A timeslot is divided into 156.25 symbol periods. The period between bursts appearing in successive timeslots is termed the guard period. GSM downlink uses four different types of burst: normal burst, synchronisation burst, frequency correction burst, and dummy burst, as shown in Fig. 2 [12]. The normal and dummy bursts are most commonly used. The structures of these two bursts are very similar with a total duration of 148 bits, leaving a guard period equivalent in duration to 8.25 bits. Universal in the centre of the normal and dummy bursts is a 26 bit-long training sequence defined as modulating bits with states according to the training sequence code [12] for cell identification.

2.2 Signal waveform and properties

In Singapore, the equivalent isotropically-radiated power (EIRP) for a normal GSM base station is usually less than 50 W (47 dBm) with a cell coverage range radius of, at most, 2 km. The GSM base station antenna system usually employs three planar antennas covering a sector of 120° each for improving the overall base station capacity and coverage.

The GSM base station transmits waveforms encoded with either speech or data signals over a frequency carrier having a channel spacing of 200 kHz. The RF transmission is in continuous short burst format with a burst period of 557 µs and a duty cycle of 95% (148/156.25 bits). The modulation scheme used in GSM is Gaussian minimum shift keying (GMSK) with a normalised filter bandwidth time bit period of 0.3 [13]. This modulation makes it more immune to noise than amplitude shift keying (ASK). Figure 3 depicts the time domain of a GSM carrier using a complex sampling rate of 200 kHz where the guard period between bursts can be prominently seen.

A single bit in a timeslot corresponds to a duration of 3.692 µs giving a modulating data rate of 270.833 kbit/s. Thus, with a normalised filter bandwidth time bit period of 0.3, the theoretical carrier bandwidth of the GSM signal is approximately 81.3 kHz. Figure 4 illustrates the power spectrum of a GSM carrier signal. Unlike TV and FM broadcast signals, where the bandwidth changes according to the signal information, the effective bandwidth of a GSM carrier signal is practically constant.

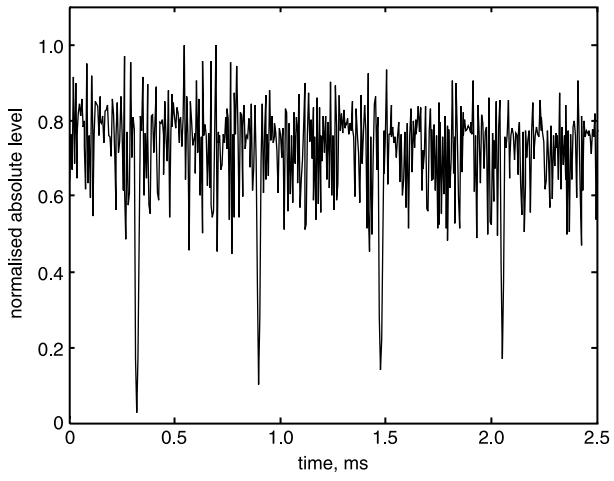

Fig. 3 *GSM signal in time domain*

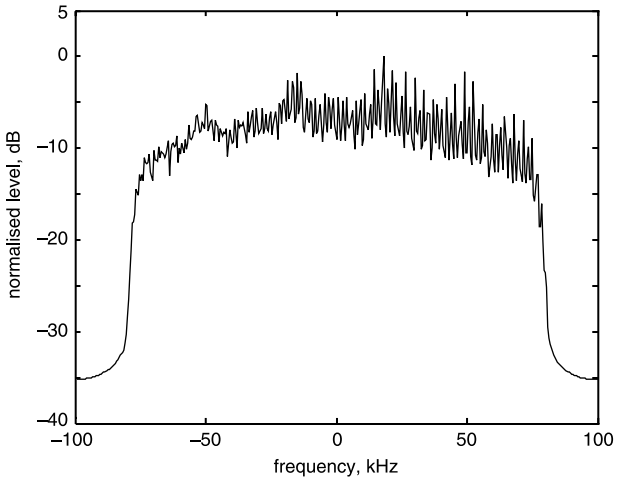

Fig. 4 *Power spectrum of GSM signal*

2.3 Passive radar design considerations

In the application of bistatic GSM-based passive radar, range resolution is inversely related to the bandwidth of the GSM signal B and bistatic angle β as

$$\Delta R = \frac{c}{2B\cos(\beta/2)} \tag{1}$$

where c is the velocity of light. ΔR is the minimum range requirement for target separation assuming that the two targets are co-linear with the bistatic bisector. For the theoretical carrier bandwidth of 81.3 kHz, the best achievable range resolution is 1.845 km (where $\beta = 0°$).

Doppler resolution is determined by the total coherent integration time (CIT) given by

$$\Delta f_d = \frac{1}{T} \tag{2}$$

Subsequently, velocity resolution can be derived as

$$\Delta V = \frac{\lambda}{2T\cos(\beta/2)} \tag{3}$$

where λ is the wavelength of the GSM carrier signal. It is noted that T has no relationship with the GSM signal/waveform properties. With a CIT of 0.2 s, Δf_d is calculated to be equal to 5 Hz and can distinguish the velocity of 0.82 m/s for $\beta = 30°$.

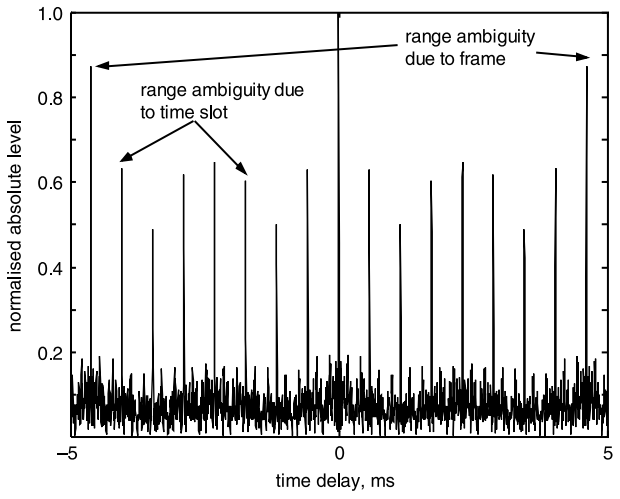

Fig. 5 *Autocorrelation function of GSM signal*

Range resolution is determined by the bandwidth of the GSM signal and frequency resolution is determined by the total duration for the coherent processing; both properties are independent of each other. Thus, given the small bandwidth of a GSM carrier signal (81.3 kHz), it is therefore insufficient to provide an acceptable range resolution. However, by increasing the CIT, a GSM signal can achieve good Doppler resolution, making the GSM-based passive radar very suitable for moving target indication applications.

The repetitive modulating signal contained in bursty-type GSM transmission is responsible for the range and Doppler ambiguities inherent in the GSM signal as a radar waveform. Range and Doppler ambiguities are calculated as $c \cdot T_p/2$ and $1/T_p$ respectively where T_p is the time slot/burst duration of 577 µs. In GSM transmission, each time slot/burst is partially correlated to the next owing to the 26 bit training sequence included in most of the transmitted burst. This means that the passive radar system will suffer from range ambiguity at multiples of 86.55 km and Doppler ambiguity at multiples of 1733 Hz. In addition, one or several successive frames may consist of similar burst information (such as frequency correction burst) and generate more Doppler ambiguity components corresponding to the multiples of frame duration, i.e., 217 Hz, 108 Hz, 54 Hz, etc.

In most practical cases, the range ambiguity is trivial since detection at such range is not achievable owing to the maximum transmit power, line of sight (LOS) distance, etc. On the contrary, the Doppler ambiguity is of great concern since the ambiguity does not cover the whole Doppler frequency of interest. Fortunately, because of the mere partial frame correlation, this significantly alleviates the problem of strong target ambiguity and in most practical cases, the target ambiguity is not evidently observed in the result plots. The autocorrelation function of the GSM carrier signal is shown in Fig. 5, which reveals the range resolution and range ambiguity of the GSM waveform. The Doppler ambiguity is not shown as it is dependent on the similarity of the coded data in each transmission burst/frame.

3 Implementation of an experimental GSM-based passive radar

3.1 System architecture

GSM-based passive radar consists of two separate but co-located antennas/receivers to receive the direct path reference signal from the GSM base station and echo signal

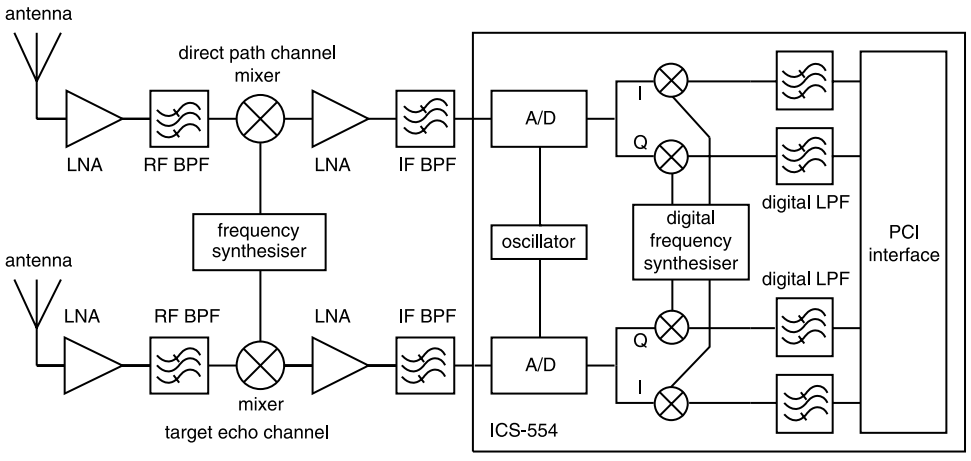

Fig. 6 *Architecture of experimental GSM-based passive radar system*

reflected from targets. For the receivers, several modules with different architectures have been developed and evaluated [8]. The final system is based on a two-channel single conversion superheterodyne receiver with intermediate frequency (IF) sampling. The digital IF signal is down-converted to baseband by a tunable digital down-converter (DDC) module that was integrated in a high performance ADC card and the I/Q data is saved continuously into the PC hard disc. Figure 6 shows the system architecture. Detailed component information will be outlined in the Sections that follow.

3.2 Antenna

Two identical special corner antennas tuned to the GSM downlink frequency band were developed and constructed for the reception of direct path signals from the GSM base station and the echo returns off the target. The special corner antenna uses a brass monopole as the radiator and aluminum panels as reflectors, which is easy to fabricate and install. Figures 7 and 8 show a photograph of the two corner antennas and the simulated radiation pattern, respectively. The antenna has a half-power azimuth beamwidth of 22.4° with a gain of 15.9 dBi and sidelobe level of −20.42 dB. It can be noted that the simulated elevation beamwidth, as in Fig. 8, has two lobes but this phenomenon is not important for ground-moving target detection. The measured azimuth radiation pattern and gain in an open area are conformal to the simulated results.

Fig. 7 *Photograph of two self-made corner antennas*

3.3 Receiver front end and IF stage

Following the antenna, a low noise amplifier (LNA) amplifies the received RF signal with a wide passband. The frequency band pre-selector, which is a low-loss bandpass filter (BPF), selects the desired GSM downlink frequency band. Next, the frequency mixer heterodynes the desired GSM carrier signal to an IF of 21.4 MHz, which was chosen based on the fact that the ADC acquisition card is able to digitise the GSM signal at this

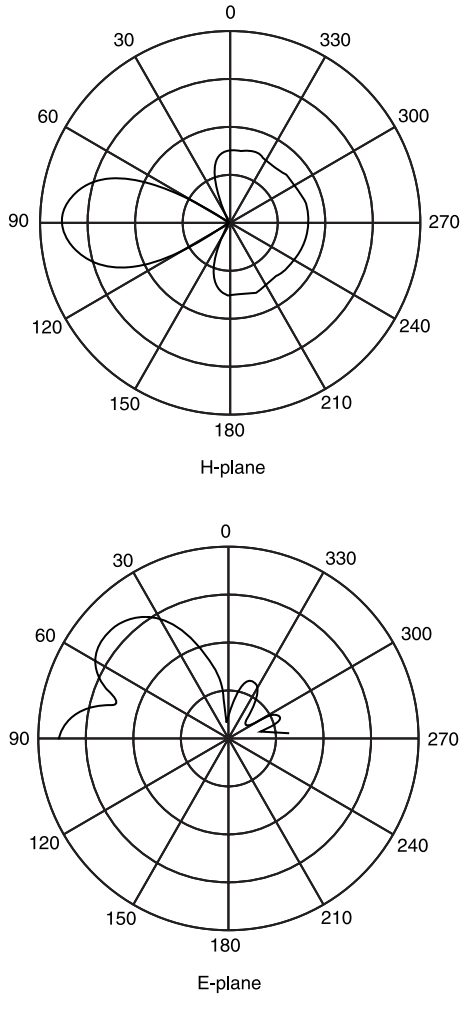

Fig. 8 *Simulated radiation pattern of corner antenna in H-plane and E-plane*

IF; cheap commercial IF BPFs are also readily available at this frequency.

A frequency synthesiser is utilised to generate the two synchronised local oscillator (LO) signals to the mixer in each receiver chain with low phase noise. The mixer IF output drives another LNA, prior to the IF BPF, to provide sufficient gain for the GSM carrier signal to achieve the full dynamic range of the ADC. This LNA actually accounts for the loss in the mixer in addition to the IF BPF, which is employed to filter out all undesired frequencies to prepare the carrier signal at 21.4 MHz for sampling.

3.4 Data acquisition

The data acquisition card used to digitise the direct path and scattered target channel signals is a PCI-based card ICS-554 from Interactive Circuits and Systems Ltd. The ICS-554 is a 4-channel, 14-bit A/D module with DDC capability, which provides approximately 84 dB of dynamic range and the maximum sampling rate can be up to 105 MHz. In the GSM-based passive radar, the ICS-554 samples the two channels of IF signals using a fixed sampling rate of 100 MHz synchronised with the LO synthesisers in the two signal chains. These digitised IF data then go into the DDC module where they are quadraturely down-converted to baseband. The down-converter is designed to maintain over 115 dB of spur-free dynamic range and over 100 dB of out-of-band rejection. Finally, after down-converting and data decimation, the output data rate is 200 kHz per I/Q channel for both the direct path and scattered target echo signal. The data streams are saved continuously onto the PC hard disc.

4 Signal processing algorithms for moving target detection

4.1 Signal processing scheme

Once the pure direct path reference signal from the direct path channel and pure target echo signal from the target echo channel are acquired, target detection can be implemented easily by applying cross-ambiguity coherent processing [14]. Unfortunately, in practical applications, both the direct path and target echo channels will contain undesired multipath interferences that distort the direct path and target echo signals significantly. Therefore, signal correction is necessary for both channels before the cross-ambiguity coherent processing. The overall signal processing scheme associated with the GSM-based passive radar is illustrated in Fig. 9.

4.2 Constant modulus algorithm for channel equalisation

First, to remove the multipath interferences and obtain the pure direct path reference signal, channel equalisation should be applied to the direct path channel signal. In the case of passive radar applications, a conventional trained adaptive algorithm cannot be used because it depends on prior knowledge of the training sequence. In this case, blind adaptive channel equalisation algorithms are suitable. Among all blind equalisation schemes, probably the most successful and practical is the constant modulus algorithm (CMA). This makes use of a prior knowledge that the complex representation of the signal has, in the absence of multipath, a constant instantaneous modulus or envelope. Physically, the CMA adjusts the filter tap weights so to reduce the variation of the signal envelope, thereby also removing undesired multipath corruption. Owing to the limitation of paper length, the detailed processing steps of the CMA based channel equalisation technique will not be listed and can be found in [15].

4.3 Least mean square based adaptive direct path/clutter cancellation

For the target signal in the target echo channel, the major problem encountered is that the strong direct path signal will also be received by the target echo antenna via its sidelobes. This is in addition to the surrounding terrain and buildings that also produce unwanted clutter returns. The magnitude of the direct path signal is usually several tens of dB stronger than the magnitude of the target echo signal. Therefore, this will seriously influence the target detection. To suppress the direct path interference received by the target echo antenna in addition to other clutter returns, optimally weighted, delayed versions of the direct path reference signal should be subtracted from the received target echo signal, based on the least mean square error (LMS) criterion. Suppose $\boldsymbol{V}$ is a reference signal matrix where each column is a unique, delayed copy of the direct path signal

$$\boldsymbol{V} = \begin{bmatrix} v(1) & v(0) & v(-1) & & v(-P+2) \\ v(2) & v(1) & v(0) & & v(-P+3) \\ \vdots & \vdots & \vdots & \cdots & \vdots \\ v(N) & v(N-1) & v(N-2) & & v(N-P+1) \end{bmatrix} \tag{4}$$

where each $v(k)$, $k = 1, \cdots, N$, is a sample of the digitised direct path signal, and P is the number of cancellation weights to be calculated, which corresponds to the anticipated maximum range over which the multipath is dominant. The digitised target signal is defined by

$$\boldsymbol{U} = [u(1), u(2), \cdots, u(N)]^T \tag{5}$$

It can be easily derived that the optimal weight vector should be

$$\boldsymbol{W} = (\boldsymbol{V}^H \boldsymbol{V})^{-1} \boldsymbol{V}^H \boldsymbol{U} \tag{6}$$

If the multipath clutter can be ignored, i.e. only considering the direct path signal from the GSM base station, the weight factor calculation can be simplified as

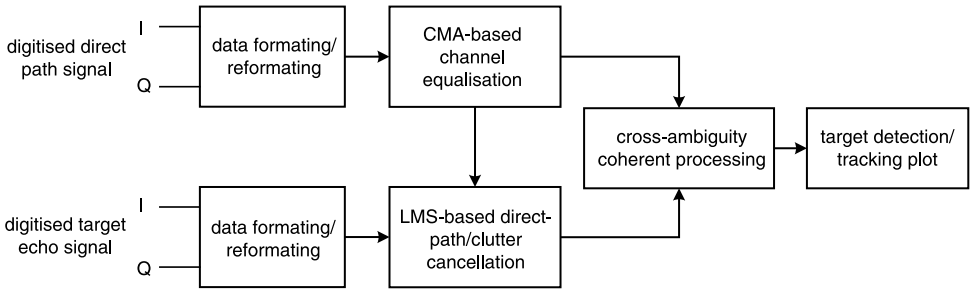

Fig. 9 *GSM-based passive radar system signal processing scheme*

$$w = \frac{\langle \boldsymbol{V}^H \cdot \boldsymbol{U} \rangle}{\|\boldsymbol{V}\|^2} = \frac{\sum_{k=1}^{N} v^*(k) \cdot u(k)}{\sum_{k=1}^{N} |v(k)|^2} \quad (7)$$

where $\boldsymbol{V}$ is the non-delayed direct path signal

$$\boldsymbol{V} = [v(1), v(2), \cdots, v(N)]^T \quad (8)$$

4.4 Cross ambiguity coherent processing

The natural generalisation of the cross correlation coherent process is essentially the complex ambiguity function [14], which is the matched filter response to the joint time-delay and Doppler-shifted version of the GSM signal it is matched to and is given as

$$A(\tau, f_d) = \int_{-\infty}^{+\infty} s_1(t) \cdot s_2^*(t+\tau) \cdot \exp(-j2\pi f_d t) dt \quad (9)$$

where $s_1(t)$ and $s_2(t)$ are the received target echo signal (after direct path/clutter cancellation) and direct path signal (after channel equalisation) respectively. τ and f_d are, respectively, the time-delay and Doppler frequency shift parameters to be searched for the values that cause $|A(\tau, f_d)|$ to peak. For $f_d = 0$, the above cross ambiguity function reduces to the cross correlation function. For $f_d \neq 0$, the computation can be viewed as a correlation carried out after first translating all the spectrum in $s_2(t+\tau)$ by an amount of f_d, with peak values occurring when the value for f_d exactly compensates for the Doppler frequency from the corresponding component in $s_1(t)$. Thus, the cross ambiguity coherent processing can produce an integrated range-Doppler map depicting the detected target range and Doppler frequency shift.

Considering the poor range resolution (1.845 km) of the GSM waveform, the GSM-based passive radar may be more suitable for Doppler detection and tracking when observing the moving targets at short range, i.e., within the first resolution cell. In this case, the cross ambiguity processing can be simplified appropriately as

$$A(f_d) = \int_{-\infty}^{+\infty} s_1(t) \cdot s_2^*(t) \cdot \exp(-j2\pi f_d t) dt \quad (10)$$

This can be used to produce a plot depicting the integration time against the target Doppler frequency shift map to implement the target Doppler tracking.

5 Experimental results

5.1 Geometrical configuration

In order to evaluate the performance and capability of the GSM-based passive radar hardware system and associated signal processing scheme, field experiments were conducted using a selected operational GSM base station in near-rural surroundings. Figures 10 and 11 show the trial site and geometrical configuration respectively. In this configuration, one antenna points to the GSM base station and the other points to the open main road or the slip road under foliage. Different types of targets moving along the two roads were measured. Note that as a result of the poor range resolution of the GSM signal, all ground-moving targets measured are located within the first range cell and the focus is on target Doppler frequency tracking. In addition, our experimental sites are open areas without many buildings and tall structures and the multipath interferences are not critical. Thus, disregarding the channel equalisation in the direct path channel does not have a significant effect on the processing results. The GSM downlink spectrum at the location of the passive radar was measured using a spectrum analyser with a commercial monopole antenna, illustrated in Fig. 12. The carrier frequency channel at 938 MHz (indicated by the arrow) was chosen for the experiments. For all result plots, unless specially stated otherwise, the adopted coherent integration time is 0.2 s.

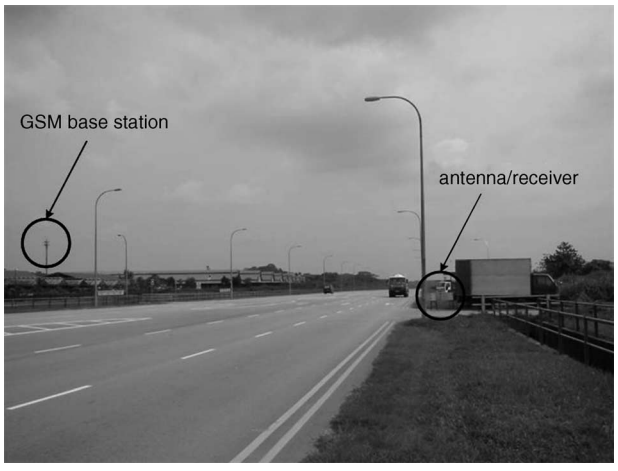

Fig. 10 *Photograph of experimental site for ground-moving target measurements*

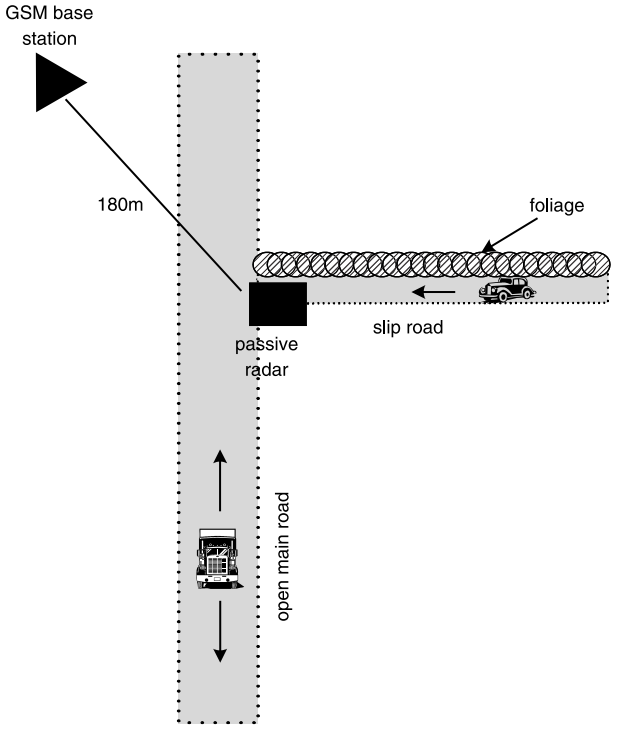

Fig. 11 *Geometrical configuration for ground-moving target measurements*

5.2 Vehicle measurements on the open main road

First, a cooperative stationary truck started off at the location of the passive radar and accelerated steadying to approximately 50 km/h in an opening direction. Figure 13 shows the corresponding Doppler tracking result. In this Figure, the direct path signal energy at zero Doppler was suppressed completely and the increasing negative Doppler frequency trace of the cooperative truck was clearly detected and tracked.

It should be noted that besides the target Doppler track and remaining DC component near zero Doppler, some RF interferences can also be found at certain Doppler

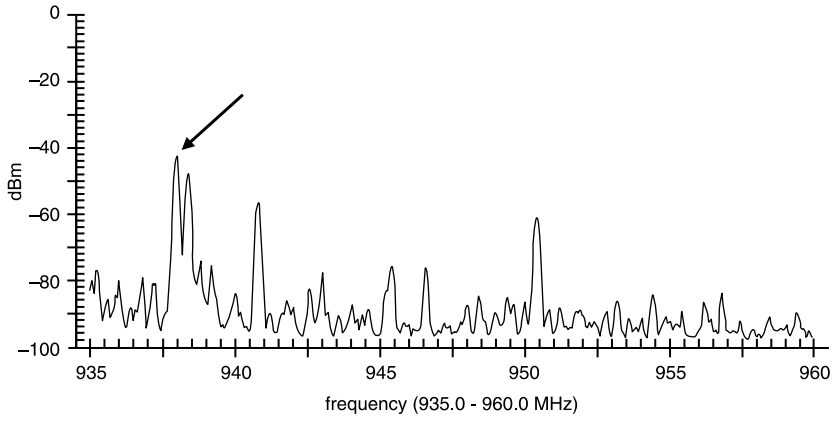

Fig. 12 *Spectrum at experimental site for ground-moving target measurements*

frequencies. These RF interferences may be due to the following two reasons. First, the modulation structure of the GSM signal has some inherent periodicities. As mentioned, the training sequence in each burst (duration of 577 μs) induces the Doppler ambiguity of 1733 Hz. Similarly, one or several successive frames may consist of similar burst information (such as frequency correction burst) and generate more Doppler ambiguity components corresponding to the multiples of frame duration, i.e. 217 Hz, 108 Hz, 54 Hz, etc. These Doppler ambiguities are also a form of RF interferences and their potential frequency values can be predicted. Signal fluctuation owing to multipath propagation is another probable cause of RF interferences in the resulting integration time-Doppler frequency map. The amplitude fluctuation in both the received direct path and target echo signal may contain some periodicities that show up prominently as RF interferences at frequencies according to the signal fluctuation period. The potential locations of these RF interferences caused by multipath signal fluctuation are generally difficult to predict.

Experiments have also been conducted for other different types of ground-moving targets such as car and motorcycle in which their Doppler frequency are also successfully detected and tracking. Some results can be found in [9] and will not be further elaborated in this paper.

5.3 Vehicle measurements on the slip road under foliage

In the previous experiment, both the radar antennas and moving vehicle are within the line of sight of the GSM base station. This next measurement assesses the target detection performance of the GSM-based passive radar under foliage penetration. A cooperative truck started off at the location of the passive radar and moved at a uniform speed of 15 km/h along the slip road under the foliage, outside the direct line of sight of the GSM base station. It can be calculated that the target Doppler frequency will be 25 Hz for the case of monostatic configuration ($\beta = 0°$). Considering the small bistatic angle in this measurement configuration, the measured target Doppler can be estimated to be slightly smaller than 25 Hz. Figure 14 shows the integration time-Doppler frequency plot, in which the target Doppler frequency at 20 Hz is very prominent. This result proves the potential foliage penetration capability of the GSM-based passive radar.

5.4 Human motion measurements

In addition to the ground-moving vehicles, some small target (low RCS) measurements, such as human motion, were also conducted using the same configuration as above.

The ground truth for this measurement has a human running towards the passive radar from around 100 m away and making a U-turn when reaching the location of antennas before returning to the starting point. Figure 15 shows the Doppler frequency tracking result, where the Doppler frequency induced by the human body can be clearly identified. In addition, some Doppler distortion/spreading caused by arm swinging can also be seen.

Next, a man stood 3 m away from the radar antennas and swung his arms in the following sequence: 0–10 s with no motion, 11–30 s with arms swinging slowly, 31–50 s with arms swinging more rapidly and 51–60 s with no motion again. The observation result in Fig. 16 indicates identical correspondence to the event sequence stated.

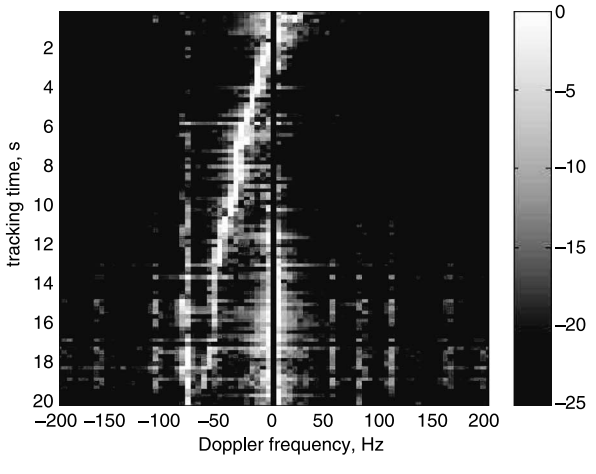

Fig. 13 *Doppler tracking result for cooperative truck on main road*

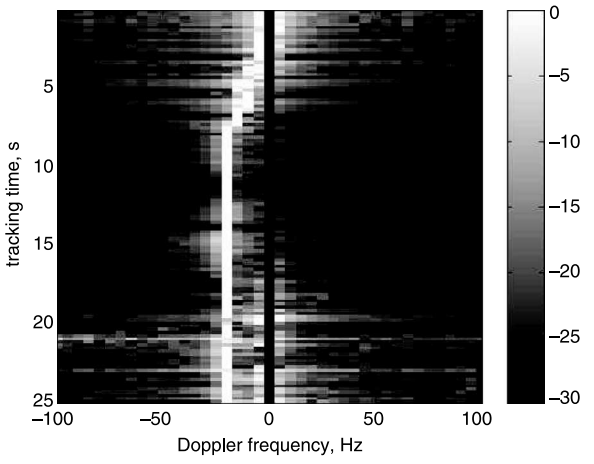

Fig. 14 *Doppler tracking result for cooperative truck on slip road under foliage*

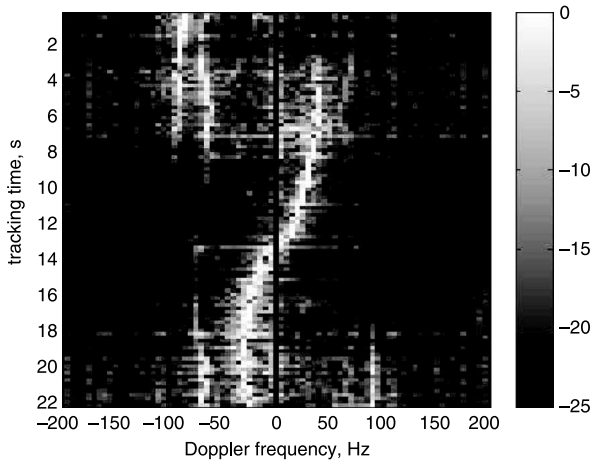

Fig. 15 *Doppler tracking result for cooperative running human on main road*

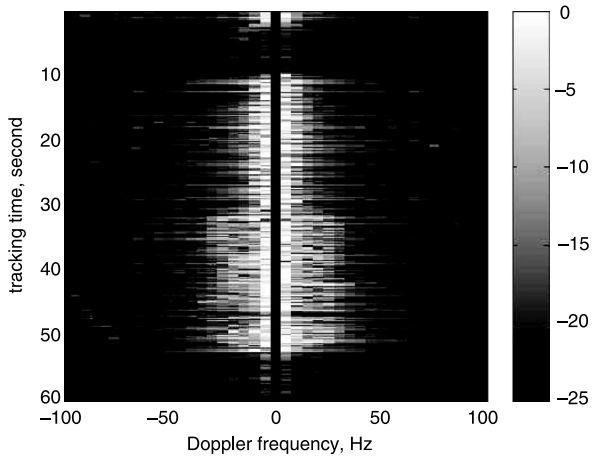

Fig. 16 *Doppler tracking result for cooperative stationary human with arm swing on main road*

5.5 Discussion on the operation range

In the above experiments, the maximum operation range of the GSM-based passive radar prototype is not at all impressive, i.e. several hundred meters to 1 km for ground-moving vehicles. The probable cause is mainly a result of the dense honeycomb cell configuration (to support higher capacity) in Singapore where the GSM base station operates with low transmitting power (less than 50 W). According to the information from the mobile communication service provider, the maximum coverage of a cell in Singapore is less than 1.5 to 2 km. Comparatively, the actual operation range of the GSM-based passive radar prototype achieved in the field experiments is probably reasonable. As a matter of fact, in many other bigger countries, a rural cell may have a coverage range of up to 30 km and the EIRP of a GSM base station may be as high as 640 W. For this reason, the range performance for the same system in such a cell will be definitely much more superior.

6 Conclusion and future work

The research work in is paper verifies the feasibility of using a GSM downlink signal as a radar waveform. Based on the theoretical analysis, a low-cost GSM-based passive radar prototype was developed and numerous field experiments were conducted. From the processing results illustrated in Section 5, there is no doubt that the GSM-based passive radar has the potential capability to detect different types of ground-moving targets, especially for the target Doppler frequency tracking.

Although many positive results have been obtained, it must be pointed out that these are just preliminary results and there is still more work for continuation and improvements. First, to achieve better performance for direct path signal cancellation and interference/clutter suppression, a compact array antenna and relevant multichannel receiver is under development, in addition to the adaptive digital beamforming algorithms. Second, the potential capability of GSM-based passive radar for ship and aircraft target detection needs to be verified and more advanced signal processing techniques, such as time-frequency representations, may be used to enhance the performance of target detection and Doppler frequency tracking. Some work on this is currently under way and a more detailed analysis of the experimental results will be discussed in future papers. In addition, in the GSM communication system, there are multiple base station transceivers for the coverage of a large area. This feature of such an abundance of illuminators of opportunity enables the feasibility for design and development of a multistatic passive radar network. Undoubtedly, the reliability and performance of target detection and tracking will benefit greatly from the multistatic radar network using multiple transmitters and receivers.

7 References

1 Griffiths, H.D.: 'From a different perspective: principles, practice and potential of bistatic radar'. Int. Conf. on Radar, Adelaide, Australia, September 2003, pp. 1–7
2 Sahr, J.D., and Lind, F.D.: 'The Manastash Ridge radar: a passive bistatic radar for upper atmosphere radio science', *Radio Sci.*, 1997, **32**, (6), pp. 2345–2358
3 Griffiths, H.D., and Long, N.R.W.: 'Television-based bistatic radar', *IEE Proc., Radar Sonar Navig.*, 1986, **133**, (7), pp. 649–657
4 Howland, P.E.: 'Target tracking using television-based bistatic radar', *IEE Proc., Radar Sonar Navig.*, 1999, **146**, (3), pp. 166–174
5 Griffiths, H.D., Garnett, A.J., Baker, C.J., and Keaveney, S.: 'Bistatic radar using satellite-borne illuminators of opportunity'. IEE Int. Conf. on Radar, Brighton, UK, October 1992, pp. 276–279
6 Cherniakov, M., Nezlin, D., and Kubik, K.: 'Air target detection via bistatic radar based on LEOS communication signals', *IEE Proc., Radar Sonar Navig.*, 2002, **149**, (1), pp. 33–38
7 Tan, D.K.P., Sun, H., Lu, Y., and Liu, W.: 'Feasibility analysis of GSM signal for passive radar'. IEEE Radar Conf., Huntsville, USA, May 2003, pp. 425–430
8 Sun, H., Tan, D.K.P., and Lu, Y.: 'Design and implementation of an experimental GSM based passive radar'. Int. Conf. on Radar, Adelaide, Australia, September 2003, pp. 418–422
9 Tan, D.K.P., Sun, H., and Lu, Y.: 'Ground moving target measurements using a GSM based passive radar'. Int. Conf. on Radar Systems, Toulouse, France, October 2004, 6P-RCMT-141
10 ETSI EN 300 910, 'Digital cellular telecommunications system (Phase 2+); radio transmission and reception'. GSM 05.05 version 8.5.1 Release 1999, November 2000
11 ETSI TS 100 573, 'Digital cellular telecommunications system (Phase 2+); physical layer on the radio path: general description'. GSM 05.01 version 8.4.0 Release 1999, August 2000
12 ETSI EN 300 908, 'Digital cellular telecommunications system (Phase 2+); multiplexing and multiple access on the radio path'. GSM 05.02 version 8.5.1 Release 1999, November 2000
13 ETSI EN 300 959, 'Digital cellular telecommunications system (Phase 2+); modulation'. GSM 05.04 version 8.1.2 Release 1999, February 2001
14 Stein, S.: 'Algorithms for ambiguity function processing', *IEEE Trans. Acoust. Speech Signal Process.*, 1981, **29**, (3), pp. 588–599
15 Treichler, J.R., and Agee, B.G.: 'A new approach to multipath correction of constant modulus signals', *IEEE Trans. Acoust. Speech Signal Process.*, 1983, **31**, (2), pp. 459–471